

APPLICATION OF HIGHER-ORDER HEAT FLUX MODEL FOR PREDICTING TURBULENT METHANE-AIR COMBUSTION

by

Ali ERSHADI and Mehran RAJABI-ZARGARABADI*

Department of Mechanical Engineering, Semnan University, Semnan, Iran

Original scientific paper

<https://doi.org/10.2298/TSCI181110415E>

The present study addresses a new effort to improve the prediction of turbulent heat transfer and NO emission in non-premixed methane-air combustion. In this regard, a symmetric combustion chamber in a stoichiometric condition is numerically simulated using the Reynolds averaged Navier-Stokes equations. The Realizable $k-\epsilon$ model and discrete ordinate are applied for modelling turbulence and radiation, respectively. Also, the eddy dissipation model is adopted for predicting the turbulent chemical reaction rate. Zeldovich mechanism is applied for estimating the NO emission. Higher-order generalized gradient diffusion hypothesis is employed for predicting the turbulent heat flux in turbulent reactive flows. Results show that the higher-order generalized gradient diffusion hypothesis model is capable of predicting temperature distribution in good agreement with the available experimental data. Comparison of the results obtained by the simple eddy diffusivity and HOGGDH models shows that applying the higher-order generalized gradient diffusion hypothesis significantly improves the over-prediction of NO emission. Finally, the average turbulent Prandtl number for the non-premixed methane-air combustion has been calculated.

Key words: methane combustion, turbulent heat flux, turbulent Prandtl number, higher-order generalized gradient diffusion hypothesis

Introduction

Turbulent reaction flows have a wide range of applications in different areas such as home, military and industrial uses [1]. In general, the accurate prediction of scalar and vector fields in turbulent combustion is very challenging and requires solving 3-D unsteady turbulent reaction flow field. Given the widespread use of turbulent combustion, many researches have been conducted experimental and numerical investigations. The use of methods for pollution reduction and flame control [2, 3], swirl flows [4], as well as the use of stabilizer jets [5] are examples of research studies regarding these reaction flows. In most of the numerical simulations, modelling of turbulent flows has been performed using the RANS equations.

Fang and Xiang [6] studied the effect of fluctuation on the production of NO in a swirl combustion chamber. They considered second-order models for multiply sentences of fluctuations in the rate of reaction \overline{KY} and validated the obtained results for temperature and nitrogen oxides using the available experimental results [7]. Numerical studies have been performed by Amini *et al.* [8] using different turbulence models for optimizing the performance of a combustor. Their results show that the non-linear third order $k-\epsilon$ turbulence model shows a favorable agreement with the experimental results.

* Corresponding author, e-mail: rajabi@semnan.ac.ir

In some recent studies, methods of direct numerical simulation (DNS) [6, 9] and large eddy simulation (LES) [10] have been performed for modelling the turbulent air-fuel combustion. Due to the high computational cost required for the DNS and LES approach, the RANS model is widely used in engineering applications.

Turbulent scalar flux vectors are created by averaging the energy equation in turbulent flow. Given the importance of temperature property in combustion flows, turbulent heat fluxes would have a significant effect on predicting combustion characteristics. The model of simple eddy diffusivity (SED) with constant turbulent Prandtl number is the simplest turbulent heat flux model that has been used in many studies [11]. In this model, by assuming a constant turbulent Prandtl the turbulent heat flux vector has been considered to be aligned with the temperature gradient. This model has revealed a poor approximation and can cause errors in predicting turbulent heat flux vector [12-15].

It has been shown that the turbulent Prandtl number has a considerable effect on predicting the temperature distribution in turbulent flows [13-15]. It is found that the estimation of turbulent Prandtl number is varied from 0.1-10 [13, 14]. The presented relations regarding the determination of turbulent Prandtl number have been provided based on functions of different parameters such as molecular Prandtl number, eddy viscosity, viscosity and turbulence kinetic energy [15-17].

Several advanced models have been proposed for modelling the turbulent heat flux vector. These models include the two equations models [18] explicit algebraic [12, 19, 20] and implicit algebraic [21] models. Algebraic or second order models are more applicable than one and two-equation models and provide an acceptable accuracy. Daly and Harlow [12] presented a simple algebraic explicit model called generalized gradient diffusion hypothesis (GGDH) for the turbulence flux vector that was defined as a function of Reynolds stress tensor, temperature gradient and turbulence kinetic energy. Suga and Abie [20, 22] proposed a second order model as the high-order generalized gradient-diffusion model (HOGGDH). The formulation of HOGGDH model was based on the GGDH model with the difference that the effect of a higher level of turbulent flow (Reynolds stresses) to predict the turbulent heat flux has been applied in this model. The HOGGDH model has more computing time and accuracy than those of GGDH. Wikstrom [19] provided a comprehensive algebraic and explicit model for the heat flux turbulence that consists of four main sentences including production, molecular distribution and turbulence, pressure and heat flux dissipation rate.

In previous studies various algebraic models (SED, GGDH, HOGGDH) have been performed for modelling turbulence heat flux in flows such as, the heat transfer of impinging jet [23], cooling flows [24-26] and pipe flows [27]. Results of previous studies show that using higher order algebraic models lead to increase of prediction accuracy of temperature distribution, especially in areas with severe (high) gradients.

In the numerical simulations of turbulent combustion flows based on RANS, the simple model of SED with assuming constant turbulent Prandtl number has been used. Studies show that the SED model with constant turbulent Prandtl number, especially in areas with high temperature gradient is inefficient [28, 29].

Therefore, using of high order models of turbulent heat flux can lead to an increase of the prediction accuracy of temperature and combustion characteristics. The main objective of this paper is to determine how turbulent Prandtl number changes in a non-premixed gas fuel combustion chamber. In this regard a high order model of turbulent heat flux is applied for the methane-air combustion. The obtained results are compared with available experimental results and the SED model. In the end, as well as calculation of turbulent Prandtl number, its changes

in various sections of the chamber are investigated and finally, the turbulent Prandtl number is proposed in the turbulent gas fuel combustion flow.

Problem description

The present study, is performed on the basis of the experimental research of Zhou and Chen [7]. The combustor is considered as a symmetric, co-flowing turbulent methane diffusion jet flame. Methane is injected through an 8 mm diameter jet nozzle, D_1 . The air jet is impinged from a circular nozzle with 30 mm diameter, D_3 . Air/fuel mixture is injected to a cylindrical combustor with diameter D_f and length L_f . The flame configuration is illustrated in fig. 1. The operating conditions used in the present study is summarized in tab. 1.

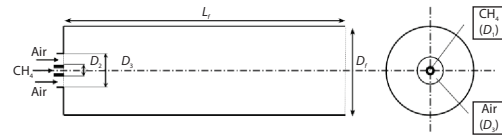


Figure 1. Schematic view of the combustion chamber [7]

Table 1. Operational conditions of the combustor

Geometry [m]				
Fuel inlet zone, D_1	from $r = 0.000$		to $r = 0.004$	
Wall between fuel & air inlet, D_2	from $r = 0.004$		to $r = 0.005$	
Air inlet zone, D_3	from $r = 0.005$		to $r = 0.015$	
Furnace diameter, D_f	0.08			
Furnace length, L_f	0.9			
Inlet and outlet boundary conditions	Fuel	Air	Out	Wall
Mass-flow rate [m^3h^{-1}]	0.8932	8.9	Pressure Outlet	–
Turbulent intensity [%]	5	5	2	–
Temperature [K]	300	300	300	500
Pressure [kPa]	101.3	101.3	101.3	–
Y_{O_2}	–	0.2315	0.2315	–
Y_{N_2}	–	0.7685	0.7685	–
Y_{CH_4}	1	–	–	–

Governing equations and numerical models

The governing equations for the combustion modelling are steady-state conservation equations for mass, momentum, species and energy. The fluid is assumed Newtonian and incompressible with variable density. The effect of gravity can be neglected [30] and the ideal gas behavior is assumed for reactants and products of the combustion. The Favre-averaged transport equation can be expressed [30]:

$$\frac{\partial(\bar{\rho}\tilde{u}_i)}{\partial x_i} = 0 \quad (1)$$

$$\frac{\partial(\bar{\rho}\tilde{u}_i\tilde{u}_j)}{\partial x_i} = -\frac{\partial\bar{p}}{\partial x_j} + \frac{\partial}{\partial x_i} \left[\mu \left(\frac{\partial\tilde{u}_i}{\partial x_j} + \frac{\partial\tilde{u}_j}{\partial x_i} \right) - \overline{\rho u'_i u'_j} \right] \quad (2)$$

$$\frac{\partial(\bar{\rho}c_p\tilde{u}_i\tilde{T})}{\partial x_i} = \frac{\partial}{\partial x_i} \left[k \left(\frac{\partial \tilde{T}}{\partial x_i} \right) - \bar{\rho}c_p \overline{u_i T'} \right] + S_{\text{reac}} + S_{\text{rad}} \quad (3)$$

$$\frac{\partial(\bar{\rho}\tilde{u}_i\tilde{Y}_n)}{\partial x_i} = \frac{\partial}{\partial x_i} \left[\bar{\rho}D_{n,m} \left(\frac{\partial \tilde{Y}_n}{\partial x_i} \right) - \bar{\rho}\overline{u_i Y'_n} \right] + R_n \quad (4)$$

The last terms at the right-hand side of eqs. (3) and (4) represent the thermal source (reactions and radiation), $S_{\text{reac}} + S_{\text{rad}}$, and, R_n , the reaction rate of species. Reynolds stress tensor as well as the vector of the turbulent heat flux and mass flux terms are important terms that should be modeled.

Turbulent flow model

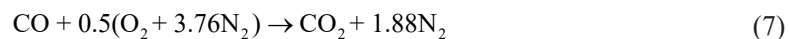
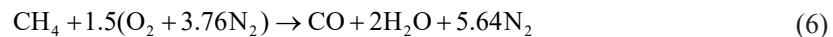
In an incompressible flow, the components of Reynolds stress tensor are related to the average velocity gradients using the Boussinesq hypothesis [31]:

$$\overline{\rho u'_i u'_j} = -\mu_t \left(\frac{\partial \tilde{u}_i}{\partial x_j} + \frac{\partial \tilde{u}_j}{\partial x_i} \right) + \frac{2}{3} \bar{\rho} k \delta_{ij} \quad (5)$$

Saqr and Wahid [32] compared several turbulence models and demonstrated that the $k-\varepsilon$ realizable model can be adopted as the best approach to model the turbulent flame. In the present study, the $k-\varepsilon$ realizable model is applied for modelling the turbulent flow. The equations and details about the model formulation are given in [31, 32].

Combustion modelling

The methane/air combustion involves complex chemical reaction mechanism. Different reaction mechanisms have been proposed for methane/air combustion [1]. In the present study, a two-step chemical reaction mechanism is used for the methane-air combustion chemical reactions process, which is described [33]:



This mechanism has been widely used by researchers in recent years [28-30]. It has been shown that this mechanism is capable to predict the major species of combustion.

Turbulence-combustion interaction

Due to fluctuating characteristics of the flow, the EDM is employed to investigate the chemical-turbulence interactions. This model is applicable for turbulent combustion flows with high reaction rates. The ED model takes the minimum value of the reaction rate evaluated using the following eqs. (8) and (9) as the local average reaction rate [34]:

$$R_n = 4v'_{i,r} M_{\omega,n} \bar{\rho} \frac{\varepsilon}{k} \min \left(\frac{\tilde{Y}_R}{v'_{R,r} M_{\omega,R}} \right) \quad (8)$$

$$R_n = 2v'_{i,r} M_{\omega,n} \bar{\rho} \frac{\varepsilon}{k} \frac{\sum_p \tilde{Y}_R}{\sum_j v''_{j,r} M_{\omega,R}} \quad (9)$$

Turbulent heat flux models

The SED, presented by Daly and Harlow [11], is the simplest algebraic model for the turbulent heat flux vector. This model can be written:

$$\overline{u_i T'} = -\frac{\nu_t}{Pr_t} \frac{\partial \tilde{T}}{\partial x_i} \quad (10)$$

Based on experimental results, the turbulent Prandtl number converges to a constant value (commonly 0.85) for the near-wall flows. Launder [12] showed that more accurate results can be achieved by incorporating Reynolds stress components for modelling the turbulent heat flux. The [11] presented the model of GGDH. In this model, a higher order of Reynolds stress effect was considered to represent the turbulent heat flux which can be written:

$$\overline{u_i T'} = -C_\theta \tau \overline{u_i' u_j'} \frac{\partial \tilde{T}}{\partial x_j} \quad (11)$$

where τ is the turbulence time scale, which is typically defined as $\tau = k/\varepsilon$ and C_θ is the constant of the model and is equal to 0.3 [11] or 0.25 [35]. Suga *et al.* [36] carried out modifications on the model by defining the model coefficient, C_θ , as a function of turbulent stress.

Suga and Abie [22] presented a new model based on GGDH model, called HOGGDH, for flows in the areas close to the wall. Indeed, HOGGDH completes GGDH model by taking into account a higher level of turbulence stress which can be written [37]:

$$\overline{u_i T'} = -C_\theta \tau \left(\frac{\overline{u_i' u_k'} \cdot \overline{u_k' u_j'}}{k} \right) \frac{\partial \tilde{T}}{\partial x_j} \quad (12)$$

In this model, C_θ and τ are defined in accordance with GGDH model, and the components of Reynolds stress tensor are computed with eq. (5).

Modelling of radiation

In this study, discrete ordinates (DO) model was adopted to take into account thermal radiation heat flux effects. Discrete ordinates model is suitable for thin optical thickness problems ($aL < 1$) [38]. For flow into the combustion chamber, L corresponds to diameter of chamber and a is the absorption coefficient (range between 0.01-0.1 m^{-1}). In the current study, according to the diameter of the chamber and the absorption coefficient range, the problem can be considered as optically thin, and hence, DO model is applicable in the present study. The radiation intensity transport equation and the relations relevant to DO model are fully presented in [38].

Modelling of NO_x

The destruction and formation of NO are included in the reactions associated with thermal, prompt and fuel NO mechanisms. Depending on the type of fuel (CH₄), the prompt and fuel NO can be safely ignored [5]. In the present study, to evaluate the production of NO, is determined by the extended Zeldovich mechanism [1]:



Assuming a quasi-steady ($d[\text{N}]/dt \cong 0$), NO formation rate is obtained [5]:

$$\frac{d[\text{NO}]}{dt} = 2k_1[\text{O}][\text{N}_2] \frac{\left(1 - \frac{k_{-1}k_{-2}[\text{NO}]^2}{k_1[\text{N}_2]k_2[\text{O}_2]}\right)}{\left(1 + \frac{k_{-1}[\text{NO}]}{k_2[\text{O}_2] + k_3[\text{OH}]}\right)} \quad (16)$$

where k_i is the coefficient of the reaction rate in eq. (13). The concentration of [O], [OH] radicals are determined under partial equilibrium assumption.

Numerical solution

On the basis of the experimental study [7] the modeled gas combustion chamber is symmetric. Hence a quarter of the chamber is considered for numerical solution and the side planes have been presumed symmetric. A structured non-uniform mesh was generated for the computational domain. Figures 2(a) and 2(b), shows a close-up of the present grid for the region near the fuel-air injection. A smaller grid size was utilized in the reaction zone near the interfaces of the fuel and air to provide further accuracy for the solution of the flow field. Several meshes have been tested in the present study for examining the grid independence solution. The selected grid was composed of 163000 cells for the grid independence solution.

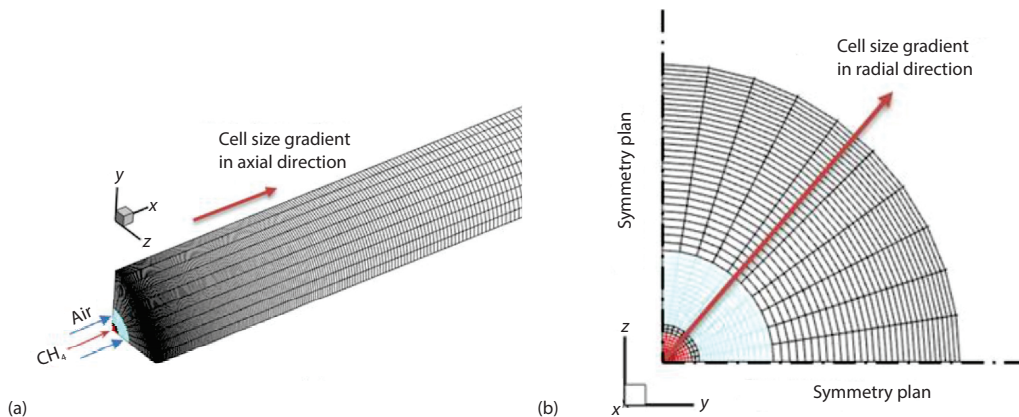


Figure 2. Grid mesh distribution of the combustor; (a) a general view of the computational domain and (b) details of the grid at the inlet

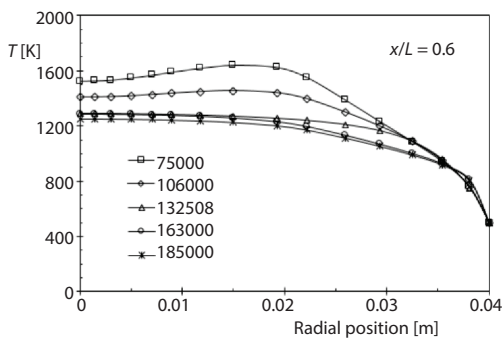


Figure 3. Effect of grid refinement size on temperature profile

The grid independence study has been done by refining the multi-block structured, quadrilateral cells over the computational domain. It can be found from fig. 3 that with the grid refinement from 163000-185250 elements, the maximum changes in the temperature is less than 2%. Hence, the grid configuration with 163000 cells is chosen for further computations.

The governing equations have been solved using the steady solver based on finite volume method by ANSYS-FLUENT CFD

software [38]. In order to apply the HOGGDH model, a user defined function (UDF) was developed in C programming language. In the written UDF code, the HOGGDH model is defined as a source term in the energy equation.

Second order upwind scheme was used to discretize the equations and the SIMPLE algorithm was adopted for the coupling between velocity and pressure. Convergence of simulation is achieved when the root mean square residuals was taken equal to 10^{-7} for energy and NO conservation equations and 10^{-4} for all other equations. The boundary and operating conditions used in the present study is summarized in tab. 1. The standard wall function is also applied to take into account the near-wall treatment.

Results and discussions

In the present paper, the second-order turbulent heat flux model has been applied for a turbulent diffusion combustion with methane fuel. The present numerical simulation is compared with the available experimental data [7]. Figure 4 shows the contour of temperature predicted by SED and HOGGDH turbulent heat flux models. The maximum temperature predicted by the SED and HOGGDH models are 2000 K and 1650 K, respectively. According to the fig. 4, the high temperature zone in the HOGGDH model is much smaller than the SED model. It can be found that applying the second-order HOGGDH model leads to the lower predicted temperatures.

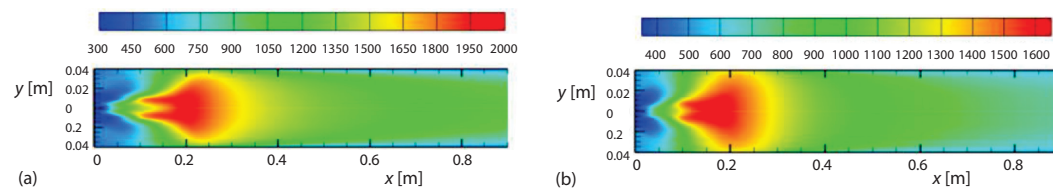


Figure 4. Contour of the static temperature at symmetry plan; (a) the SED model and (b) the HOGGDH model

The distributions of temperature along the central axis for two different turbulent heat flux models (SED and HOGGDH) are compared with the experimental data in fig. 5. The temperature profile near the inlet is in very good agreement with the experimental data. However the temperature profile for downstream of the combustor shows significant deviations. It should be mentioned that the reacting zone in the combustion chamber is located near $x = 0.2$ m where the choice of the turbulence-chemistry interaction model plays an important role. The temperatures predicted by the SED model are found to be in better agreement with the experimental data. The distribution of temperature using second order turbulent heat flux model is in a good agreement with experimental data in the downstream section. The average deviations of the predicted axial temperature by SED and HOGGDH models are equal to 28% and 7.8%, respectively.

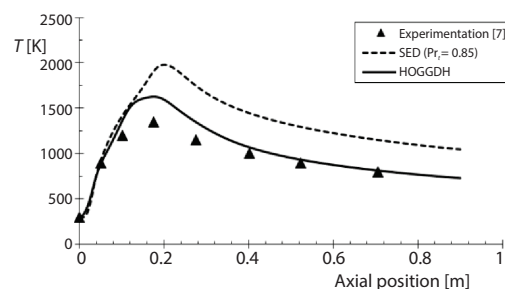


Figure 5. Centerline temperature distributions predicted by different turbulent heat flux models

In figure 6, the radial distribution of temperature are compared with the experimental data [7] at four various distances ($x/L = 0.05, 0.11, 0.2,$ and 0.3). Based on the profiles of

primary sections ($x = 0.05, 0.11, \text{ and } 0.2$), SED model overestimates the temperature in the central zone of the chamber and it underestimates the temperature in the near the wall region. This phenomena is due to the more heat diffusion in second order models compared to the first order models. It can be concluded that applying the HOGGDH heat flux model causes a significant effect on the predicted local temperature. The temperature distributions predicted by the SED model give a higher gradient specially in the center of combustion chamber, ($r/D < 0.02$). This means that the SED model fails to capture the heat diffusion in high temperature region

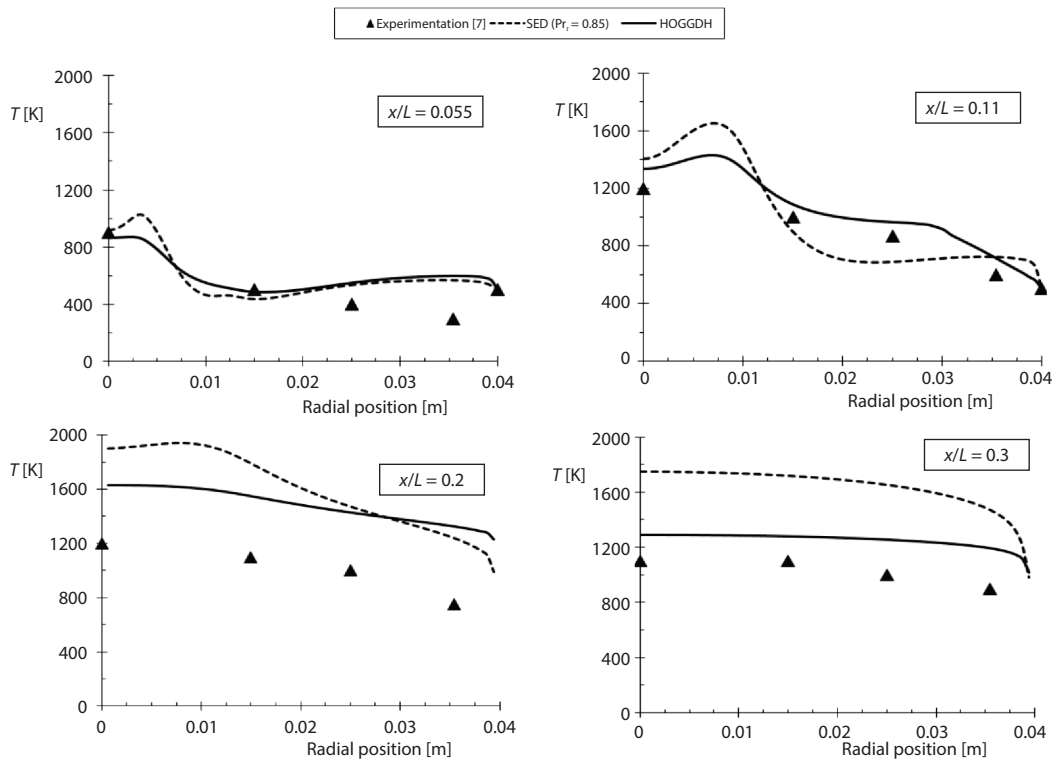


Figure 6. Temperature profiles predicted by different turbulent heat flux models

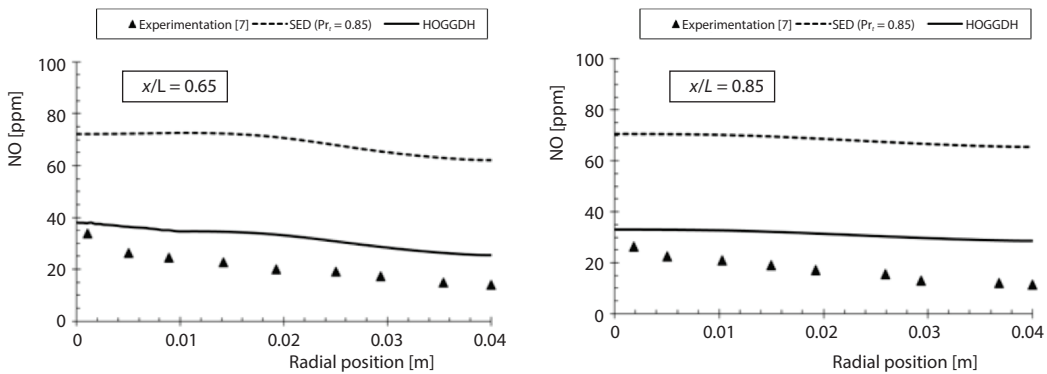


Figure 7. The NO mole fraction at different axial distance

[20, 22, 23]. However, lower temperature gradients have been predicted by the HOGGDH model in the same region. Figure 6 shows that temperature profiles predicted by HOGGDH model are in better agreement with the experimental data [7].

Figure 7 depicts the thermal NO values at three sections of the chamber for the different turbulent heat flux models. In all three sections, the predicted NO using SED model is substantially higher than the value of HOGGDH model and also the measurements, owing to the over prediction of the maximum temperature of SED model. The NO formation values predicted by the HOGGDH model are fairly close to the available experimental data [7]. By applying the HOGGDH model, the average deviation of the NO production reduces from 200% to less than 25%.

Turbulent Prandtl number

With negligible body force and negligible viscous dissipation, turbulent Prandtl number can be expressed in accordance with the following equation [24]:

$$Pr_t = \frac{\varepsilon_M}{\varepsilon_H} \quad (17)$$

where equation ε_H is the heat eddy diffusivity, ε_M – the momentum eddy diffusivity. Assuming a 2-D flow on a flat plate, ε_M and ε_H are defined [23]:

$$-\overline{u'v'} = \varepsilon_M \frac{\partial \overline{u}}{\partial y}, \quad -\overline{u'T'} = \varepsilon_H \frac{\partial \overline{T}}{\partial y} \quad (18)$$

With substituting eq. (18) in the eq. (17), the following relation is achieved:

$$Pr_t = \frac{\overline{u'v'} \frac{\partial \overline{T}}{\partial y}}{\overline{u'T'} \frac{\partial \overline{u}}{\partial y}} \quad (19)$$

Based on Reynolds analogy, the turbulent Prandtl number would be converged to a constant value which generally is in the order of unity and is considered as 0.85 [11]. Numerical simulation and experimental results show that the turbulent Prandtl number can go through significant variations even in simple flows [39]. Prandtl number distribution using HOGGDH model at different radial positions are displayed in fig. 8. It is apparent from the figure that Prandtl number at the center of the combustion chamber is about 0.2 and it augments gradually with moving towards the wall. An increase of axial distance toward downstream results in a reduction in average Prandtl number. Previous studies showed that the turbulent Prandtl number in problems such as channel flow and film cooling flow varies from 0.1-1 [13] and 0.3-2.2, respectively, [24].

The mean radial turbulent Prandtl number along the axis is illustrated in fig. 9. It can be perceived from the figure that the predicted turbulent Prandtl number using the HOGGDH model varies from 0.2-1.9. Due to the decrease of temperature gradient and turbulent stress-

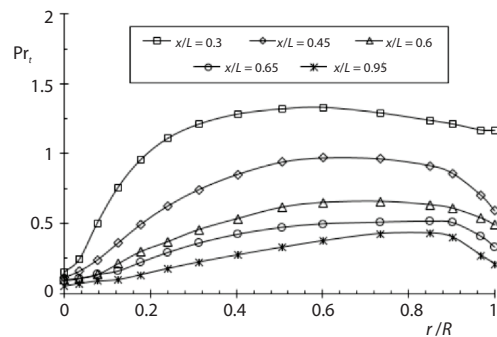


Figure 8. Predicted turbulent Prandtl number by HOGGDH model

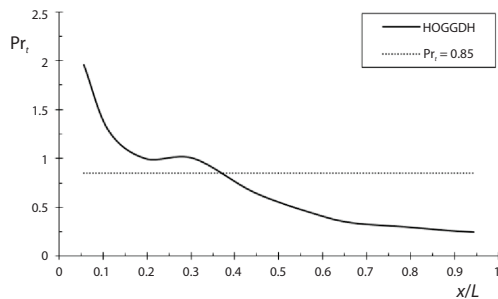


Figure 9. Mean turbulent Prandtl number along the chamber

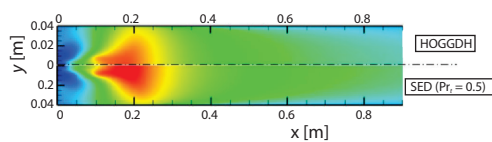


Figure 10. Temperature contour predicted by HOGGDH and SED ($Pr_t = 0.5$) models

The radial distributions of temperature predicted by SED ($Pr_t = 0.5$) and HOGGDH models are compared with the experimental data [7] in fig. 11. This figure implies that the assumption of $Pr_t = 0.5$ could provide a good agreement with experimental results. According to fig. 4, the reaction zone is located near $x = 0.2$ m. In the downstream zone ($x > 0.4$ m) the mixing process allows to reach a uniform temperature profile.

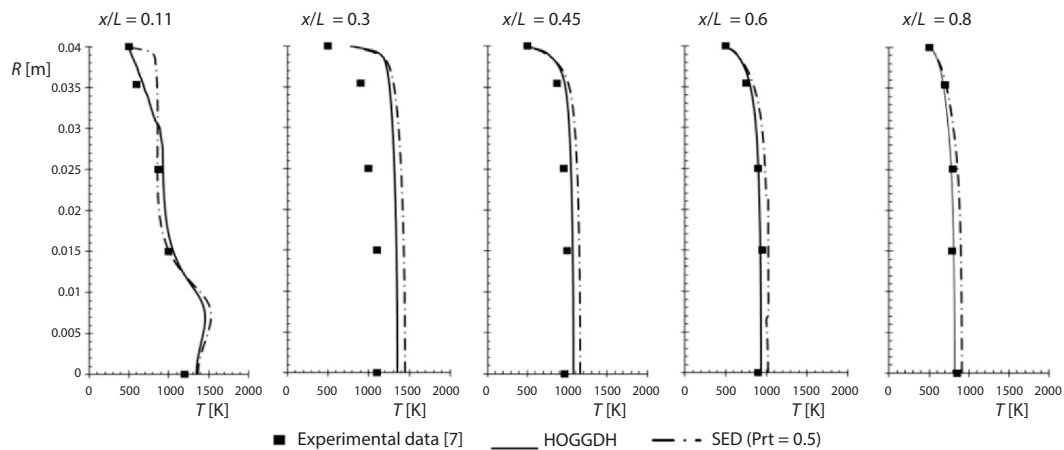


Figure 11. Comparison of temperature distribution predicted by HOGGDH and SED ($Pr_t = 0.5$)

Conclusion

The main purpose of the present study is to estimate the variation of turbulent Prandtl number in the methane-air combustion. The numerical simulation is carried out for a symmetric diffusion flame. The realizable $k-\varepsilon$ model and EDM are adopted for predicting the behavior of turbulent flow and combustion, respectively. In order to model the turbulent heat flux vector, two algebraic models, including the SED and HOGGDH models, have been applied. Results

es, turbulent Prandtl number decreases with the distance from the entry zone. The profiles of figs. 8 and 9 show that assuming the constant value of 0.85 for turbulent Prandtl number is not realistic and this parameter significantly changes in different region of the combustion chamber. Therefore, one of the strategies for increasing the accuracy of the primary SED model in modelling the combustion flows is to modify the turbulent Prandtl number.

Based on the results of the HOGGDH model, the average value of the turbulent Prandtl number for the entire of combustion zone is equal to 0.5. The distribution of temperature predicted by the SED model ($Pr_t = 0.5$), has been compared with the HOGGDH model in fig. 10. It can be seen that, the results predicted by turbulent Prandtl number of 0.5 have a good agreement with HOGGDH model.

of the present numerical simulation show that the turbulent heat flux model plays an important role in predicting the combustion characteristics. The SED model with a constant value of 0.85 for the turbulent Prandtl number fails to predict the temperature field and NO distribution in the methane-air combustion. The HOGGDH is more accurate than the SED model due to incorporating the Reynolds stresses in calculating the turbulent heat flux vector. Comparisons between the numerical results show that the HOGGDH model gives a reasonable prediction of temperature distribution in comparison with the experimental data. Also, applying the HOGGDH model significantly improves the over-prediction of NO mole fraction distribution. The results show that, the radial turbulent Prandtl number varies from 0.2-1.9 along the combustion chamber. It is found that, for the present numerical simulation constant Prandtl number of 0.5 for the methane-air combustion leads to a better prediction of temperature distributions.

Nomenclature

a – absorption coefficient
 C_θ – model coefficient
 c_p – heat capacity
 D – diameter of combustor
 $D_{n,m}$ – diffusion coefficient, species n in ambient m
 d – fuel nozzle diameter
 k – turbulent kinetic energy
 k_{-i} – reverse reaction rate coefficient in reaction i
 k_{+i} – forward reaction rate coefficient in reaction i
 L – length of the cylindrical volume
 $M_{o,n}$ – production molecular weight
 $M_{o,R}$ – reactant molecular weight
 p – pressure
 Pr_t – turbulent Prandtl number
 R – radius
 R_n – species production/consumption rate
 S_h – heat source term
 T – temperature
 t – time
 u_i – velocity vector components
 $\overline{u'_i u'_j}$ – components of Reynolds stress tensor
 $\overline{u'_i T'}$ – components of turbulent heat flux vector
 $\overline{u'_i Y'}$ – components of turbulent mass flux vector
 Y_n – mass fraction for species n

ε_H – heat eddy diffusivity
 ε_M – momentum eddy diffusivity
 δ_{ij} – Kronecker symbol
 μ – dynamic molecular viscosity
 μ_t – dynamic turbulent viscosity
 ν_t – turbulent kinematic viscosity
 ρ – density
 τ – turbulent time scale
 $v'_{i,r}$ – stoichiometric coefficient, for reactant species i in reaction i
 $v'_{i,p}$ – stoichiometric coefficient, for product species i in reaction i

Acronyms

DNS – direct numerical solution
 EDM – eddy dissipation model
 GGDH – generalized gradient diffusion hypothesis
 LES – large eddy simulation
 HOGGDH – higher-order generalized gradient-diffusion model
 SED – simple eddy diffusivity

Other symbols

\sim – Favre average
 $\overline{\quad}$ – Reynolds average

Greek symbols

ε – heat eddy diffusivity– dissipation rate of the turbulent kinetic energy

References

- [1] Turns, S. R., Mantel, S. J., *An Introduction Combustion*, 2nd ed., McGraw Hill, New York, USA, 2000
- [2] Belocevic, S., *et al.*, Modelling of Pulverized Coal Combustion for in-Furnace NO_x Reduction and Flame Control, *Thermal Science*, 21 (2017), Suppl. 3, pp. S597-S615
- [3] Belocevic, S., *et al.*, Modelling and Optimization of Processes for Clean and Efficient Pulverized Coal Combustion in Utility Boiler, *Thermal Science*, 20 (2016), Suppl. 1, pp. S183-S196
- [4] Yichao, L., *et al.*, Combustion Characteristics of a Slotted Swirl Combustor: An Experimental Test and Numerical Validation, *International Communications in Heat and Mass Transfer*, 66 (2015), Aug., pp. 140-147
- [5] Alemi, E., Rajabi-Zargarabadi, M., Effects of Jet Characteristics on NO Formation in a Jet-Stabilized Combustor, *International Journal of Thermal Sciences*, 112 (2017), Feb., pp. 55-67

- [6] Fang, W., Xiang, X., Effect of Turbulence on NO Formation in Swirling Combustor, *Chinese Journal of Aeronautics*, 27 (2014), 4, pp. 797-804
- [7] Zhou, L. X., Chen, L. X., Studies on the Effect of Swirl on NO Formation in Methan/Air Turbulent Combustion, *Proceedings of the Combustion Institute*, 29 (2002), 2, pp. 2235-2242
- [8] Amini, B., et al., A Comparative Study of Variant Turbulence Modelling in the Physical Behaviors of Diesel Spray Combustion, *Thermal Science*, 15 (2011), 4, pp. 1081-1093
- [9] Scholtissek, A., et al., In-Situ Tracking of Mixture Fraction Gradient Trajectories and Unsteady Flamelet Analysis in Turbulent Non-Premixed Combustion, *Combustion and Flame*, 175 (2017), Jan., pp. 243-258
- [10] Irannejad, A., et al., Large Eddy Simulation of Turbulent Spray Combustion, *Combustion and Flame*, 162 (2015), 2, pp. 431-450
- [11] Daly, B. J., Harlow, F. H., Transport Equation in Turbulence, *Phys Fluids*, 13 (1970), 11, pp. 2634-2649
- [12] Launder, B. E., On the Computation of Convective Heat Transfer in Complex Turbulent Flows, *Journal of Heat Transfer (ASME)*, 110 (1988), 4b, pp. 1112-1128
- [13] Bae, Y., A New Formulation of Variable Turbulent Prandtl Number for Heat Transfer to Supercritical Fluids, *International Journal of Heat and Mass Transfer*, 92 (2016), Jan., pp. 792-806
- [14] Bae, J. H., et al., Direct Numerical Simulation of Turbulent Supercritical Flows with Heat Transfer, *Phys. Fluids*, 17 (2005), 10, pp. 105104-1-105104-24
- [15] Yamamoto, Y., Kunugi T., Modelling of MHD Turbulent Heat Transfer in Channel Flows Imposed-wall-Normal Magnetic Fields under the Various Prandtl Number Fluids, *Fusion Eng. Des.*, 109-111 (2016), Part B, pp. 1130-1106
- [16] Moffat, R. J., Kays W. M., A Review of Turbulent-Boundary-Layer Heat Transfer Research at Stanford, 1958-1983, *Advances Heat Transfer*, 16 (1984), pp. 241-365
- [17] Jones, R., et al., Improved Turbulence Modelling of Film Cooling Flow and Heat Transfer, Chapter 4: *Modelling and Simulation of Turbulent Heat Transfer*; (Eds. B. Sunden, M. Faghri), WIT Press, Southampton, UK, 2005
- [18] Nagano, Y., Shimada, M., Development of a Two-Equation Heat Transfer Model Based on Direct Simulations of Turbulent Flows with Different Prandtl Numbers, *Physics of Fluids*, 8 (1996), 12, pp. 3379-3402
- [19] Wikstrom, P. M., Derivation and Investigation of a New Explicit Algebraic Model for the Passive Scalar Flux, *Physics of Fluids*, 12 (2000), 3, pp. 688-702
- [20] Abe, K., Suga, K., Towards the Development of a Reynolds-Averaged Algebraic Turbulent Scalar Flux Model, *International Journal of Heat and Fluid-Flow*, 22 (2001), 1, pp. 19-29
- [21] Rogers, M. M., et al., An Algebraic Model for the Turbulent Flux of a Passive Scalar, *Journal of Fluid Mechanics*, 203 (1989), June, pp. 77-101
- [22] Suga, K., Abe, K., Non-linear Eddy Viscosity Modelling for Turbulence and Heat Transfer Near-Wall and Shear-Free Boundaries, *Int. J. Heat Fluid-Flow*, 21 (2000), 1, pp. 37-48
- [23] Bazdidi-Tehrani, F., Rajabi-Zargarabadi, M., Application of Second Moment Closure and Higher Order Generalized Gradient Diffusion Hypothesis to Impingement Heat Transfer, *Transactions of The CSME*, 32 (2008), 1, pp. 91-105
- [24] Rajabi-Zargarabadi, M., Bazdidi-Tehrani, F., Implicit Algebraic Model for Predicting Turbulent Heat Flux in Film Cooling Flow, *Int. J. Numer. Meth. Fluids*, 64 (2010), 64, pp. 517-531
- [25] Rup, K., Wais, P., An Application of the $k-\epsilon$ Model with Variable Prandtl Number to Heat Transfer Computation in Air-flows, *Heat Mass Transfer*, 34 (1999), 6, pp. 503-508
- [26] Mazaheri, K., et al., A Modified Turbulent Heat-Flux Model for Predicting Heat Transfer in Separating-Reattaching Flows and Film Cooling Applications, *Appl. Therm. Eng.*, 110 (2017), Jan., pp. 1609-1623
- [27] Mazaheri, K., et al., Application of a Modified Algebraic Heat-Flux Model and Second-Moment-Closure to High Blowing-Ratio Film-Cooling and Corrugated Heat-Exchanger Simulations, *Appl. Therm. Eng.*, 124 (2017), Sept., pp. 948-966
- [28] Kurreck, M., et al., Prediction of the 3-D Reacting Two-Phase Flow Within a Jet-Stabilized Combustor, *Journal Eng. Gas Turbine Power*, 120 (1998), 1, pp. 77-83
- [29] Yilmaz, I., Effect of Swirl Number on Combustion Characteristics in a Natural Gas Diffusion Flame, *Journal Energ. Resour*, 135 (2013), 4, pp. 0422041-0422048
- [30] Saqr, et al., Effect of Free Stream Turbulence on NO_x and Soot Formation in Turbulent Diffusion CH₄-air Flames, *International Communications in Heat and Mass Transfer*, 37 (2010), 6, pp. 611-617
- [31] Hinze, J. O., *Turbulence*, McGraw-Hill Publishing Co., New York, USA, 1975
- [32] Saqr, K., Wahid, M., Comparison of Four Eddy-Viscosity Turbulence Models in the Eddy Dissipation Modelling of Turbulent Diffusion Flames, *Int. J. Appl. Math. Mech.*, 7 (2011), 19, pp.1-18

- [33] Silva, C. V., *et al.*, Analysis of the Turbulent Non-Premixed Combustion of Natural Gas in a Cylindrical Chamber with and without Thermal Radiative, *Combust. Sci. and Tech.*, 179 (2007), 8, pp. 1605-1630
- [34] Magnussen, B. F., *et al.*, On Mathematical Modelling of Turbulent Combustion with Special Emphasis on Soot Formation and Combustion, *Symposium (International) on Combustion*, 16 (1977), 1, pp. 719-729.
- [35] Li, X., *et al.*, Application of Algebraic Anisotropic Turbulence Models to Film Cooling Flows, *Int. J. of Heat and Mass Transfer*, 91 (2015), Dec., pp. 7-17
- [36] Suga, K., *et al.*, Application of a Higher Order GGDH Heat Flux Model to 3-D Turbulent U-Bend Duct Heat Transfer, *Journal of Heat Transfer*, 125 (2003), 1, pp. 200-203
- [37] Ryan, K. J., *et al.*, Turbulent Scalar Mixing in a Skewed Jet in Crossflow: Experiments and Modelling, *Flow, Turbulence and Combustion*, 98 (2017), Nov., pp. 781-801
- [38] ***, Flueent, A. N. S. Y. S., Ansys Fluent, Academic Research Release, Vol. 14, 2015
- [39] Redjem-Saad, L., *et al.*, Direct Numerical Simulation of Turbulent Heat Transfer in Pipe Flows: Effect of Prandtl Number, *Int. J. of Heat and Fluid-Flow*, 28 (2007), 5, pp. 847-861